International Journal on
"Technical and Physical Problems of Engineering"
(IJTPE)
Published by International Organization of IOTPE

ISSN 2077-3528
IJTPE Journal
www.iotpe.com
ijtpe@iotpe.com

March 2013 | Issue 14 | Volume 5 | Number 1 | Pages 119-126

SHF MAGNETIC PROPERTIES OF FD RESISTOR SHELL

Sh.N. Aliyeva S.I. Aliyeva T.R. Mehdiyev

Institute of Physics, Azerbaijan National Academy of Sciences, Baku, Azerbaijan
shahla-aliyeva22@ramler.ru, jophphysics@gmail.ru

Abstract- The super high frequency ferromagnetic resonance in Ni-Zn films of different thickness and structure (Ni-Zn film) dielectric (Al screen) has been investigated in temperature interval from 300 up to 450K. The presumable interpretation of obtained investigated results is given in this paper.

Keywords: Ferromagnetic Resonance, Dielectric.

I. INTRODUCTION

The surface electromagnetic waves are excited by nonuniform magnetic field formed in ferrite by electric current flowing on metallic conductor situated on the investigated sample surface. In the absence of magnetocrystalline anisotropy, the spectrum and the structure of magnetostatic waves propagating in the film are defined by magnetodipole spin-spin interactions caused by dissipation fields appearing at magnetization oscillations in the film.

The practical interest to the study of surface electromagnetic waves is connected with the fact that their energy inversely decreases to the distance, whereas the energy of volume electromagnetic wave inversely decreases as the square of the distance from point source. This circumstance in practices essentially increases the range of communication system action and also increases their efficiency because of the fact that wave is "fixed" to the surface and "follows" on its curvature.

The present investigations are carried out with the aim of the study of the processes leading to appearance of surface electromagnetic waves in layered structures of ferrite dielectric metal [1-6] and also conditions at which the modulation instabilities caused by dispersion peculiarities of these structures appear. The well known nickel-zinc ferrite compositions of $Ni_{1-x}Zn_xFe_2O_4$ type synthesized on sol-gel technology and having wild use are used in the capacity of the ferrite material.

II. SYNTHESIS OF SOLID SOLUTIONS $Ni_{1-x}Zn_xFe_2O_4$

The micro- and nano-powders of solid solutions $Ni_{1-x}Zn_xFe_2O_4$ is carried out by the way of co-precipitation [7] of water solutions of impurities $NiCl_2$, $ZnCl_2$ and $FeCl_3$ in alkaline medium. The X-ray photos (XRD) of synthesized powders $Ni_{1-x}Zn_xFe_2O_4$ are studied on powder diffractometer D8 Advance (Brucker Ltd.) (CuK∝, λ=1.540600Å) and are given ion Figure 1. The scanning of the chosen peaks is made with the step 0.010°, measurement time 5.8 sec at temperature 25°C. As the measurements show, all investigated compositions have spinel structure. For x=0.5 the parameter values are equal: a=8.39900Å, z=8, volume=592.49Å^3, space symmetry group Fd3m. The observable plane reflections (311), (400), (422), (511) and (440) in Roentgen spectra correspond to spinel structure. The strongest reflection is observed from plane (311). The peaks (220) show on the fact that the half of Fe^{3+} ions in inverse spinels are in tetrahedral spaces and the second half of Fe^{3+} ions and Ni^{2+} ions are in octahedral spaces. The analogous results of roentgen experiments are obtained in [7].

It is found that lattice constant of "a" structure linearly increases from 8.288 up to 8.440Å, that corresponds to change interval between lattice constants $NiFe_2O_4$ and $ZnFe_2O_4$ with increase of zinc concentration in $Ni_{1-x}Zn_xFe_2O_4$. The temperature investigations in Figure 2 show that the structural changes are observed in them at two-hour annealing of synthesized microparticles. It is seen on behavior of ZnO lines with the temperature, especially after 600°C and increase of this fraction till it becomes dominating one at 1100°C. At temperatures from 900°C up to sintering temperature 1100°C, the ferrite particle sizes estimated by widening of Sherrer's maximums remain nano-dimensional ones. One can suppose that ZnO causes to sintering process acting as barrier for the particle growth. The coincidence of roentgen lines Fe_2O_3, ZnO, $NiFe_2O_4$, $ZnFe_2O_4$ with $Ni_{1-x}Zn_xFe_2O_4$ shown in Figures 1 and 2, allows us to give the following interpretation of observable maximums in spectra $Ni_{1-x}Zn_xFe_2O_4$.

Fe-edge firstly existing in pure phase of Ni-Zn ferrite decomposes on Fe_2O_3 and the mixture of Ni and Zn ferrites; ZnO part increases with sintering temperature. The line intensities observable for samples sintered at temperatures 800C and 900C show the increase of phase crystallinity ZnO. In temperature interval from 800°C up to 1100°C the nickel in $Ni_xZn_{1-x}Fe_2O_4$ ferrite presences in element form, increasing up to total quantity of nickel in the system. Average size of crystallites decreases from 8.95 up to 6.92 nm with increase on zinc concentration (Figure 3). Note that difference of Ni obtaining conditions also leads to change of crystallite sizes.

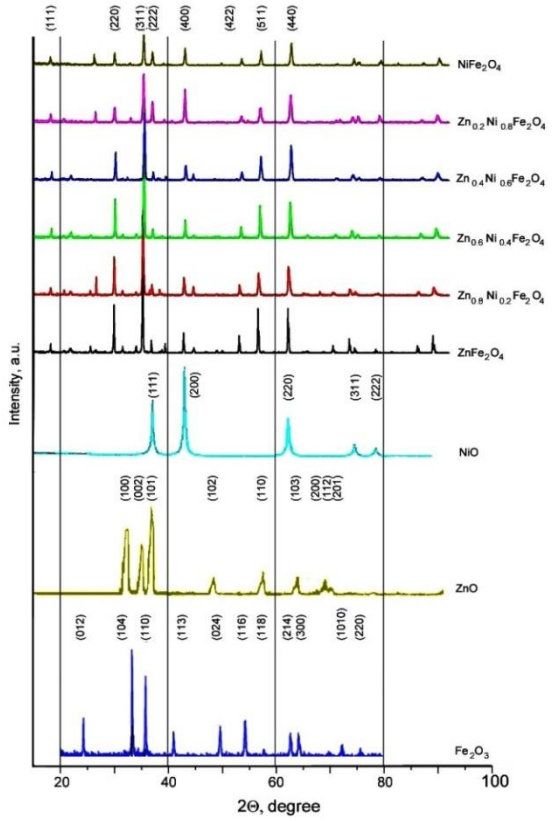

Figure 1. Indexed X-ray diffraction pattern for $Ni_{1-x}Zn_xFe_2O_4$ with x varying from 0 to 1.0 by step 0.2

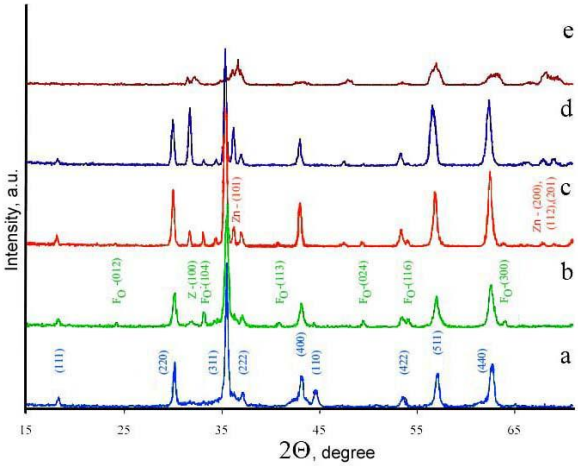

Figure 2. X-ray diffraction $Ni_{0.5}Zn_{0.5}Fe_2O_4$ at different temperatures: a is after synthesis; b is 600C; c is 800C; d is 900C; e is 1180C, F_O - Fe_2O_3; Zn - ZnO. (the experiment is carried out on X-ray diffractometer X PERT PRO, PANanalytical, Netherlands)

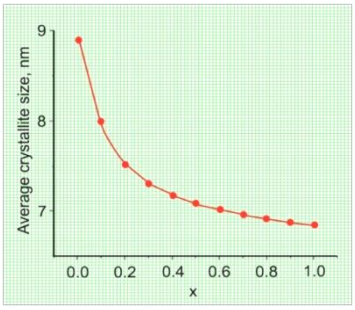

Figure 3. The average sizes of ferromagnetic particles $Zn_xNi_{1-x}Fe_2O_4$ obtained by hydrothermal method in the dependence on zinc content

III. MAGNETIC PROPERTIES OF SOLID SOLUTIONS $Ni_{1-x}Zn_xFe_2O_4$

The solid solutions $Ni_{1-x}Zn_xFe_2O_4$ of nickel-zinc ferrites are inverse spinels and present themselves the replacement solid solutions formed by two ferrites, the one of which $NiFe_2O_4$ is ferromagnetic and another $ZnFe_2O_4$ doesn't have the magnetic properties.

It is known [8] that elementary cell of ferrite spinel has the space group (O7h-F3dm). The oxygen anions form dense face-centered cubic packing containing 64 tetrahedral (A) and 32 octahedral (B) voids. In the dependence on the fact that what metallic ions and in what order take A and B voids, one can differ the direct (non-magnetic) and inverted (ferromagnetic) spinels.

The circumstance that Fe^{2+} ions are easily exchanged by bivalent Ni^{2+} and Zn^{2+} ions, explains the statistic distribution: on tetrahedral voids of Zn^{2+} and Fe^{3+} ions and octahedral voids of Ni^{2+} and Fe^{3+} ions. As the cations of different valences take the crystallographically and energetically equivalent positions in the lattice, so the electron exchange reactions carry out with activation energy $\Delta E \approx 0.05$eV.

The zinc cations in spinel structure always take tetrahedral knots. Thus, zinc introduction into crystal lattice is accompanied by rejection of ferrum ions in octahedral positions that leads to decrease of compensation of cation magnetic moments being in A and B sublattices and therefore to increase of magnetization of solid solution saturation, weakens the exchange interaction of A-O-B type that expresses in monotonous Curie temperature decrease at the increase of molar part of $ZnFe_2O_4$ in ferrite spinel composition.

In $x>0.5$ region the ion magnetic moments in tetrahedral sublattice aren't able to anti-parallel orientate the cation magnetic moments of B-lattice and the rapid decay of saturation induction, crystal anisotropy decrease and increase of initial ferrite magnetic permeability are observed. The solid solution of $Ni_{1-x}Zn_xFe_2O_4$, $x \approx 0.7$ corresponds to maximal value of magnetic permeability.

The physical model of magnetic properties of solid solutions $Zn_xNi_{1-x}Fe_2O_4$ is proposed in [8]. It is proved that till $x=0.4$ Zn^{2+} ions take only tetrahedral knots. This is also proved by the fact that in tetrahedral coordination m_{Fe}^{3+} is equal to 5. The further increase of Zn^{2+} concentration leads to situation when some part of Zn^{2+} ions begins to fill the octahedral knots. This process leads to the decrease of solid solution magnetization.

The presence of some number of Zn^{2+} ions in octahedral sublattice also explains the results of [8] in which the interaction relations between sublattices in preposition that all Zn^{2+} ions takes tetrahedral knots are calculated. The experimental results on dependence of spontaneous magnetization are presented in Figures 4-5. The "hypothetic" magnetization is defined by the following expression:

$$M_s^{hyp.} = M_s - g\left(a_x - a_{x=0.3}\right) \quad (1)$$

for all "x" values which are bigger 0.3 where M_s is experimental value for the given "x"; γ is interaction constant [8]; and a is lattice constant.

The negative γ value is explained in [9] by ratio fluctuations of Zn^{2+} and Fe^{3+} ion numbers in tetrahedral knots. The constant γ depends on lattice constant and oxygen ion position and also on interaction values Fe^{3+} - Fe^{3+}, Fe^{3+}- Zn^{2+} and Zn^{2+} - Zn^{2+} and cation distributions. The values $\gamma_{0.4}$=-1.6; $\gamma_{0.5}$=-1.65; $\gamma_{0.6}$=-1.71; $\gamma_{0.7}$=-1.79 correspond to obtained experimental results.

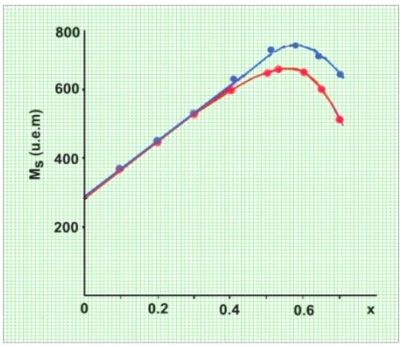

Figure 4. The dependence of spontaneous (full curve) and "hypothetic" (dotted curve) magnetizations $Ni_{1-x}Zn_xFe_2O_4$ on zinc content

It is known that at increase of ferromagnetic particle sizes, they should be one-domain ones, as the magnetostatic energy proportional to its volume decreases rapider than boundary energy between domains that is proportional to particle surface. By other hand from follows that magnetic properties of few ferromagnetic powders are defined by properties of one domain. The value of critic radius for uniaxial crystal, at which the homogeneous magnetization saves, is defined by expression [10]:

$$R_c \approx \frac{0.95}{J_s}\sqrt{\frac{10A}{Q-\frac{2K}{J_s^2}-\frac{H}{J_s}}} \qquad (2)$$

where J_s is saturation magnetization; A is exchange energy parameter; K is constant anisotropy; Q is demagnetizing factor; H is magnetic field strength . Note that particle with radius satisfying to the given equation at all field values $H > -\frac{2K}{J_S}$ remains one-domain one. At further decrease of R radius in the particle system, the probability of Brownian motion of sum magnetic moment vector increases proportionally to $\exp(E/k_BT)$ where E depends on anisotropy constant and particle volume and has the meaning the energy barrier at overcoming of which the thermal fluctuations can make the magnetic moment rotation .

In [8] it is shown that the magnetization stability in this case saves at particle sizes not less 50Å. The particle system with radiuses less than critical one behaves itself similar to paramagnetic atom ensemble having the big magnetic moment. Thus, the dependence of magnetization value of solid solutions $Ni_{1-x}Zn_xFe_2O_4$ obtained by hydrothermal method with the change of zinc concentration (Figure 5) becomes clear.

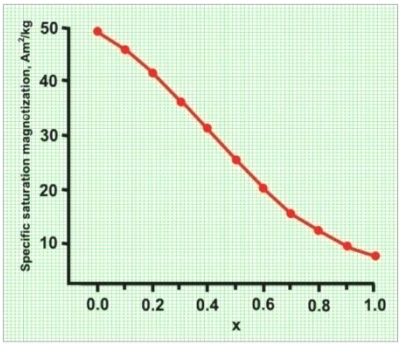

Figure 5. The dependence of solid solution magnetization $Ni_{1-x}Zn_xFe_2O_4$ obtained by hydrothermal method on zinc content

IV. COMPOSITE MAGNETIC SPECTRA (POLYMER DIELECTRIC + MIXTURE OF $Ni_{1-x}Zn_xFe_2O_4$ NANOPOWDERS)

The mechanical mixture of obtained nano-powders of solid solutions zinc-nickel ferrites is used as of filler for matrix from polymer dielectric with low dielectric constant. The concentration of ferrite powder mixture in dielectric matrix is chosen so that at the condition of particle distribution on matrix volume and absence of contacts between particles, magnetic permeability is defined by sum of magnetic permeabilities of each fraction, i.e. $\ln\mu = \sum v_i \ln\mu_i$ where μ_i is magnetic permeability, v_i is volume part of i-fraction of powder-filler in the composite. It is established that for the obtaining of these conditions the volume part of nano-powder mixture in dielectric matrix shouldn't be bigger than 0.65. The experimental dependences of mixture component magnetization $Ni_{1-x}Zn_xFe_2O_4$ where x= 0.0; 0.2; 0.4; 0.6; 0.8; 1.0 are shown in Figure 6.

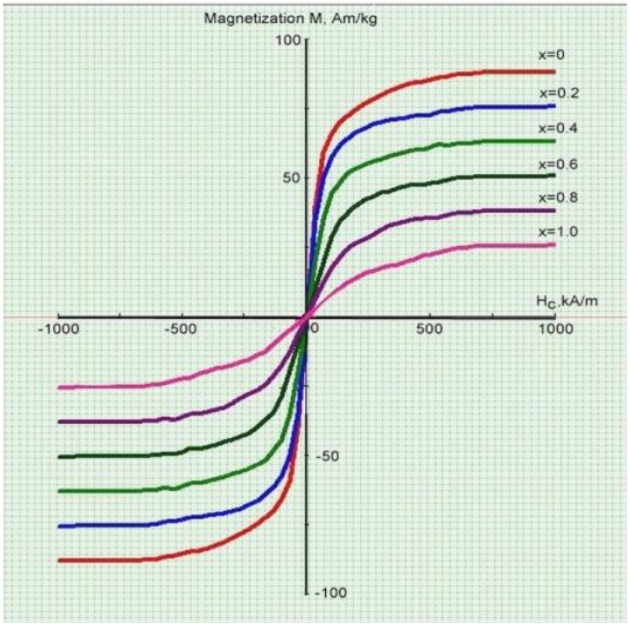

Figure 6. The dependences of nano-powder magnetization $Ni_{1-x}Zn_xFe_2O_4$ where x= 0.0; 0.2; 0.4; 0.6; 0.8; 1.0

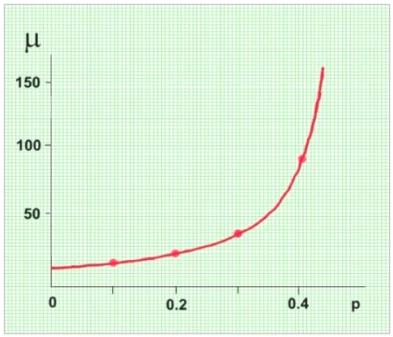

Figure 7. The dependence of composite magnetization (polymer dielectric +nano-powder mixture $Ni_{1-x}Zn_xFe_2O_4$ where x= 0.2; 0.4; 0.6; 0.8) on concentration of nano-powder mixture in polymer matrix

The oscillogram of dependence of signal $u(f)$ generated by sample on frequency of modeling magnetic field is given in Figure 9. The two resonance peaks on frequencies 23 and 177 kHz corresponding to modes of bending and planar vibrations are observed in spectrum.

The planar oscillations appear as a result of displacement of field contact on the one of sample surfaces and consequently don't characterize the investigation object. The magnetization dependence (polymer dielectric +nano powder mixture $Ni_{1-x}Zn_xFe_2O_4$ where x=0.2; 0.4; 0.6; 0.8) on nano powder volume part in polymer matrix is presented in Figure 7. The experimental dependences presented in Figures 7-8 are in well coincidence with physical model.

As analysis shows the absorption spectrum is connected with frequency dependence of ferrite permeability, frequency dependence of composite, and transition from three-dimensional character to two-dimensional one of passing current. The transition boundary frequency from three-dimension to two-dimension current character is shown by dot line l_p.

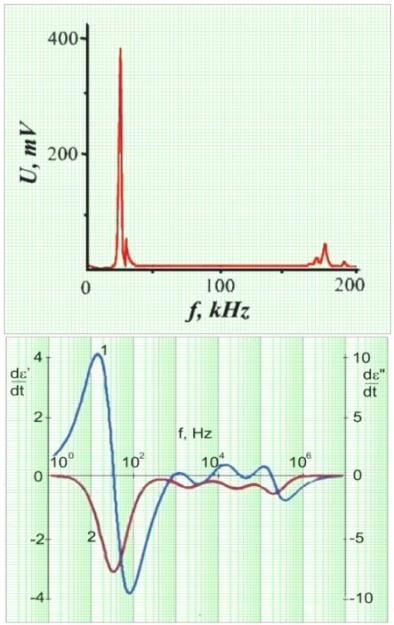

Figure 8. The sample spectrum oscillogram of $Ni_{1-x}Zn_xFe_2O_4$ in dependence on frequency of modeling magnetic field - For comparison the differential frequency dependences of actual (1) and imaginary (2) parts of dielectric constant for PVC matrix at 30°C

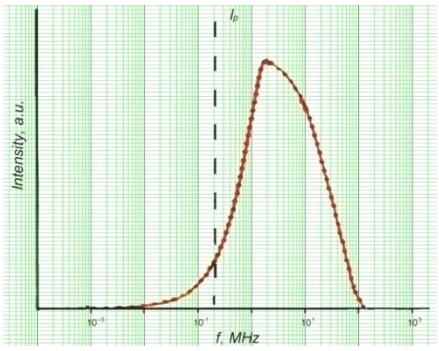

Figure 9. The absorption spectra of $Ni_{1-x}Zn_xFe_2O_4$ in frequency region from 10^2 up to $2 \cdot 10^8$ Hz

The current behavior at skin effect is defined by scale of mixed conduction system, i.e. the skin-current propagating on resistor at the skin-effect depth less than l_p will be two-dimensional character and at depth bigger than l_p it will be the three-dimensional one. The position of the scale of mixed conduction l_p as a result of dependence on component conduction coefficients $\sigma_1(\omega)$ and $\sigma_2(\omega)$ should depend on frequency ω. The calculation shows that such value of l_p, corresponds to signal frequencies higher than 200 kHz.

V. MAGNETIC RESONANCES $Ni_{1-x}Zn_xFe_2O_4$ IN SPECTRUM MICROWAVE REGION

The measurements of frequency dependence of real and imaginary components of magnetic permeability, reflection coefficient from samples in frequency range 0.3-1300 MHz are carried out with the help of measurement system of complex coefficients of transmission conjugated with computer system of signal registration and treatment. The samples positioned on metallic plane are put into measurement cell agreed with coaxial measurement tract in measurement regime of passing or reflection. The tract supplies the wave propagating of TE, TM and TEM modes. The data of validity of amplitude and phase measurements of weaken signal is achieved by introduction of set of fixed attenuators, reference terminations of corresponding frequency range.

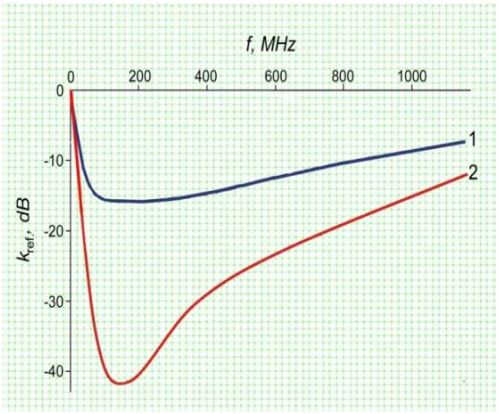

Figure 10. The frequency dependence of reflection coefficient on ferrite film surface: 1is Ni-Zn ferrite without stoichiometry disturbance; 2 is Ni-Zn ferrite with 52.5 mol% excess of iron oxide over stoichiometry

The measurements of magnetic resonance spectra are also carried out on EPR-installation of Bruker LTD (Germany), ELEXSYS-II E500 CW-EPR. The ratio of standardized sample signal Weak Pitch to the noise is 3000:1. SHF-emitter includes the powerful doubled source of Gunn diode type with super-low noise level and also the resonator with super high goodness. The installation is supplied by Herg program packet for professional EPR-spectrometry. The frequency range: from 1 up to 263 GHz.

The resonator of rectangular type in which the measured sample is positioned, is introduced in high-frequency tract supplying the measurement region from 26 up to 38 GHz. Note that in this region the dielectric constant of Ni-Zn ferrites is 13.2-14. At the absence of external magnetic field with the increase of frequency the passing coefficient increases and reflection coefficient decreases. The obtained resonant spectra coincide with results of [20] and are given in Figures 10-12.

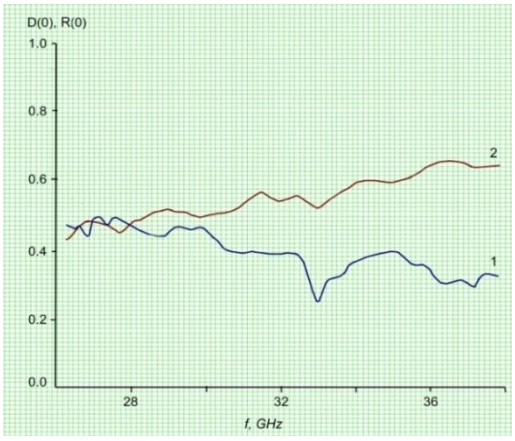

Figure 11. The spectra of passing and reflection Ni-Zn nano-composite in the presence of external magnetic field: 1 is reflection; 2 is passing

The experimental investigations of magnetic resonance in nickel-zinc nano-composite are carried out for two polarizations: $H||H^{SHF}$ and $H\perp H^{SHF}$and four particles 26, 28, 30, 32 GHz. In both polarizations the position of resonance line changes to the side of more strong magnetic fields. The values are carried out

$$d_m = \frac{|D(H)|-|D(0)|}{|D(0)|} \; ; \; k_m = \frac{|R(H)|-|R(0)|}{|R(0)|} \qquad (3)$$

where $D(H)$ is passing in external magnetic field; $D(0)$ is passing in the absence of external magnetic field; $R(H)$ is reflection in external magnetic field; $R(0)$ is reflection in the absence of external magnetic field. The spectra of passing and reflection in the absence of external magnetic field are given in Figure 11.

The magnetic resonance spectra in Zn-Ni nano-composite at passing through the composite of electromagnetic waves with frequencies: 1 is 26 GHz; 2 is 28GHz; 3 is 30GHz; 4 is 32GHz; upper figure corresponds to geometry $H||H^{SHF}$; low one corresponds to $H\perp H^{SHF}$ are shown in Figure 12. The signal amplitude for different frequencies in the second case almost linearly increases with the increase of applied magnetic field and in first case it decreases. The explanation of this effect is correctly given in [11] and connected with increasing amplitudes of resonator self-resonant frequencies with frequency increase for $H\perp H^{SHF}$ case and in $H||H^{SHF}$ case it is connected with the fact that vector direction of internal constant field approximates to the direction of external field. The differential spectra of ferromagnetic resonance (Figure 13) are obtained for sizes of $Ni_{1-x}Zn_xFe_2O_4$ particles which are equal to 10, 11, 12 and 16 nm. The investigation results are given in Table 1.

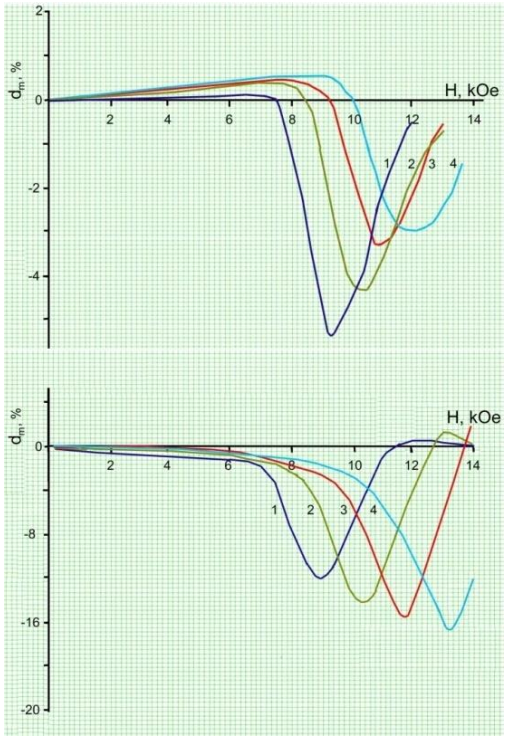

Figure 12. The magnetic resonance in Ni-Zn nano-composite at passing of electromagnetic waves through it with frequencies:1 is 26 GHz; 2 is 28GHz; 3 is 30GHz; 4 is 32GHz ; upper is $H||H^{SHF}$; low is $H\perp H^{SHF}$

Table 1. The investigation results

Size nm	Resonance field, Oe	Line width, Oe	Relaxation time, ps	Magnetization, emu/g
10	3328	836	65	9.1
11	3105	1071	48	10.5
12	3007	1666	29	19.5
16	2796	2242	20	23

From temperature EPR-investigations $Ni_{0.35}Zn_{0.65}Fe_2O_4$ (Figure 14) follows that the distribution of surface magnetic waves depends on boundary conditions. The films of different magnetizations have the different frequency pass bands of normal mode. One can excite either one or two modes in the structure in the dependence on signal frequency and parameter relation.

VI. SURFACE ELECTROMAGNETIC WAVE ON METAL-DIELECTRIC BOUNDARY

It is known that the surface magnetostatic waves propagating in single tangent magnetized ferromagnetic film [12] at the increase of signal level are stable ones in

respect to longitudinal excitations. For such wave type the modulation instability is absent in direction of excitation propagation. In [13-14] it is shown that modulation instability of surface magnetostatic waves in single ferromagnetic film can appear even at excitation of two signals on different frequencies as a result of mutual influence between two modulation stable waves.

The propagation conditions of connected volume magnetostatic waves in normal magnetized structure are investigated in [15-18]. The dispersion characteristics are studied and the appearing conditions of positive dispersion regions of rapid and low waves in linked structure.

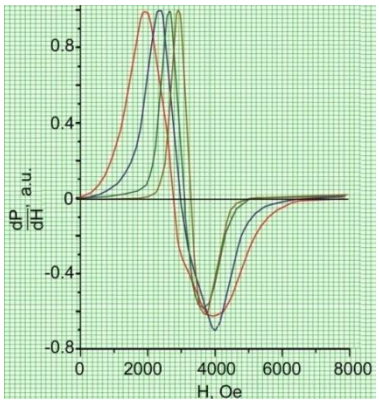

Figure 13. The differential spectra of ferromagnetic resonance of $Ni_{0.35}Zn_{0.65}Fe_2O_4$ microparticles with sizes 10, 11, 12, 16 nm

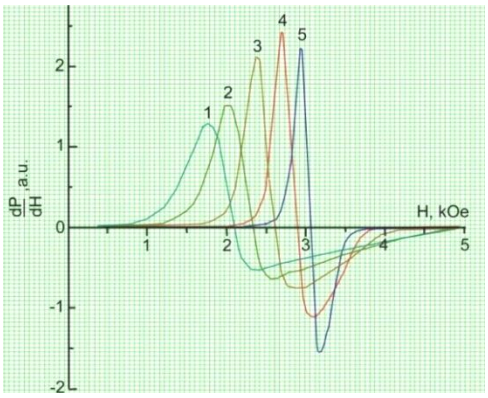

Figure 14. The temperature dependence of EPR-spectrum of $Ni_{0.35}Zn_{0.65}Fe_2O_4$: 1is 300K; 2 is 350K; 3 is 400K; 4 is 425K; 5 is 450K

The metal presence allows us to obtain any form of dispersion and also gives the possibility to control of transmission band changing it in wide limits. The analysis method of non-linear magnetostatic spin waves applied in [2] is developed in [1-6]. One of the results obtained in [3] and proved experimentally gives us a conclusion about stability condition of surface magnetostatic spin wave in respect to longitudinal excitations.

The theoretical investigations of surface magnetostatic wave instabilities are based on analyze results of Schrodinger non-linear equation solution the coefficients of which are defined from dispersion equation for magnetostatic spin wave i.e. A is impulse amplitude; $v_g = d\omega / dk$ is group velocity; $\beta_2 = d^2\omega / dk^2$ is group velocity dispersion; $\gamma = \left(\frac{d\omega}{d|A|^2} \right)_{|A|=0}$; ω is frequency; and k is wave vector of magnetostatic spin wave.

The condition of appearance of magnetostatic spin wave instability (Lighthil condition [3]) has the form: $\beta_2 . \gamma = \frac{d^2\omega}{dk^2} \left(\frac{d\omega}{d|A|^2} \right)_{|A|=0} < 0$, by other words, the condition of instability appearance is defined by dispersion law of magnetostatic spin wave group velocity. In [1, 19, 20], it is shown that the change of group velocity dispersion can be carried out with the help of metallic layer situated on some distance from ferromagnetic film. Analogically to [19-20] let's introduce the designations: d is ferromagnetic layer thickness, t is dielectric layer thickness. Let's the surface magnetostatic wave propagates along Y axis, the external magnetic field is in the structure plane and directed along Z axis.

The appearance conditions of surface electromagnetic wave in the structures dielectric-metal, dielectric-dielectric are given in [21]. First of all, this is condition that real parts of dielectric constants of both mediums should have the different signs. The medium with $\mathrm{Re}(\varepsilon)<0$ is called active one. $E(x,t)$ vector in mediums rotates clockwise describing the elliptic trajectories: flattened one for active medium and elongate one in the medium with positive ε_r.

In present paper Al is used in the capacity of metal for which: $\sigma_o = 3.7 \cdot 10^{17} s^{-1}$; $r_s/a_o = 2.07$; $l_s = 161$Å; $\Gamma = 12.5 \cdot 10^{13} s^{-1}$; $\tau = 0.8 \cdot 10^{-14}$s; $\omega_p = 2.4 \cdot 10^{16} s^{-1}$, where Γ is collision frequency with phonons, defects and other electrons; σ is conductivity; $\tau = 1/\Gamma$; ω_p is electron plasma frequency with effective mass $m^* = m_e \frac{n_o}{n_e}$; n_o is electron concentration in valent band; n_e is free electron concentration; $-r_s/a_o$ is ratio of sphere radius per one free electron to its Borovski radius; l_s is electron free length.

The polyvinylchloride, the dielectric and frequency properties of which are investigated in particular, in [16] is used in the capacity of dielectric. The calculated frequency dependences of skin-layer depth for aluminum for case when skin-layer thickness is bigger than free length are presented in Figure 16. The normal skin-effect is observed for frequencies of alternating field satisfying to $\omega\tau << 1$. The frequency region, in which the condition $1 << \omega\tau << \omega_p\tau$ is correct, corresponds to relaxation region, the oscillation frequency essentially increases the collision frequency and skin layer depth stops to depend on frequency. In some region of frequency, the skin-layer thickness can be less than free length, i.e. anomalous skin-effect should be observed [21]. For aluminum at temperature 273°K the anomalous skin-effect is seen in Figure 15.

Note that structure of frequency dependent resistor membrane is related to ferrite dielectric metal type in which the metal role plays the aluminum rod. In this case the appearing surface wave propagates along cylindrical conductor covered by dielectric shell. Let's use the theoretic conclusions of [2]. The dispersion relation $k_s(\omega)$ for all radiation range is obtained as follows:

$$\frac{\varepsilon_1}{k_1} I_0(k_2 a) K_1(k_1 a) - \frac{\varepsilon_2}{k_2} I_1(k_2 a) K_0(k_1 a) = 0 \quad (4)$$

where a is metallic rod diameter; I_0, I_1, K_0, K_1 are Bessel functions of first and second kind; $k_i = \sqrt{k_s^2 - \frac{\omega^2}{c^2}\varepsilon_i}$, $i = 1,2$.

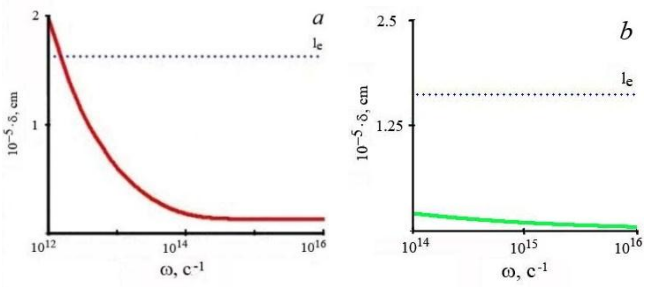

Figure 15. The depth δ (a) normal; (b) anomalous of skin effect for aluminum at 273K - l_e is free length

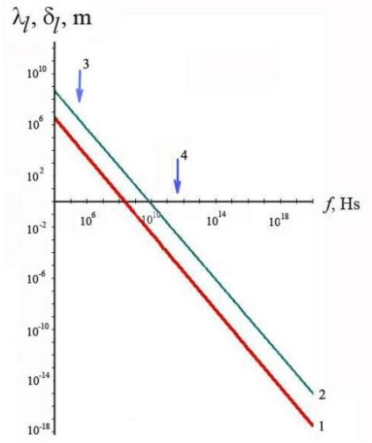

Figure 16. The frequency dependences of propagation factor λ_l of longitudinal wave (1) and damping coefficient δ_l of longitudinal wave (2), 3 and 4 are low 0.382 MHz and top $6.962 \cdot 10^5$ MHz boundaries by frequency of wave existence

In low frequency range at condition that module of complex dielectric constant is bigger than unit (i.e. Leontovich condition is carried out) and consequently, the electromagnetic wave refracted on interface practically normally propagates to the surface, for obtaining of solution of Helmgolz equation as:

$$k_1 a \frac{K_0(k_1 a)}{K_1(k_1 a)} = i Z_2 \varepsilon_1 \frac{\omega}{c} a \quad (5)$$

where $Z_2 = \left(\varepsilon_2 + i\frac{4\pi\sigma_2}{\omega}\right)^{-\frac{1}{2}}$ is active medium impedance.

For HF and SHF ranges the parameter $Z_2 \frac{\omega}{c} a$ is less than unit. The frequency dependences of propagation factor λ_l and damping coefficient δ_l of longitudinal wave are presented in Figure 16 on which the low 0.382 MHz and top 6.962×10^5 MHz boundaries of wave existence on frequency are given.

The dispersion equation of surface magnetostatic spin wave has the form [19]:

$$e^{-2kd} = \frac{(\mu - \mu_a + 1)[\mu + \mu_a + th(kt)]}{(\mu + \mu_a - 1)[\mu - \mu_a - th(kt)]} \quad (6)$$

where μ and μ_a are diagonal and non-diagonal tensor elements of ferromagnetic permeability correspondingly; k and ω are wave vector and carrier frequency of surface magnetostatic wave. From this it is followed:

$$\omega = \frac{\omega_m}{4}\alpha(1-\beta) + \frac{1}{4}\{[2(\omega_m + 2\omega_h) + \\ + \omega_m \alpha(1-\beta)]^2 - 4\omega_m^2 \beta\}^{1/2} \quad (7)$$

where $\omega_m = 4\pi\gamma M_0$, $4\pi M_0$ is ferromagnetic saturation magnetization, $\omega_h = \gamma H$, $\alpha = \exp(-2kd)$, and $\beta = \exp(-2kt)$ where γ is gyromagnetic relation. From here the wave group velocity is expressed as:

$$v_g = \frac{d\omega}{dk} = -\frac{\omega_m}{2}[d - (t+d)\beta]\alpha - \\ - \frac{\omega_m}{2}\{[d - (t+d)\beta]\alpha((2(\omega_m + 2\omega_h) + \\ + \omega_m \alpha(1-\beta))^2 - 4\omega_m^2 \beta) - 2\omega_m d\beta\} / \\ / \{(2(\omega_m + 2\omega_h) + \omega_m \alpha(1-\beta))^2 - 4\omega_m^2 \beta\}^{\frac{1}{2}} \quad (8)$$

and wave group velocity dispersion is defined as follows

$$\beta_2 = \frac{d^2\omega}{dk^2} = \omega_m[d^2 - (t+d)^2\beta]\alpha + \\ + \omega_m\{(2(\omega_m + 2\omega_h) + \omega_m\alpha(1-\beta))^2 - \\ - 4\omega_m^2\beta\}^{-3/2}\{(((2(\omega_m + 2\omega_h) + \omega_m\alpha(1-\beta))^2 - \\ - 4\omega_m^2\beta)[(2(\omega_m + 2\omega_h) + \omega_m\alpha(1-\beta)). \\ .[t^2 - (t+d)^2\beta]\alpha + \omega_m[t - (t+d)\beta]^2\alpha^2 - \\ - 4\omega_m d^2\beta]\omega_m((2(\omega_m + 2\omega_h) + \\ + \omega_m\alpha(1-\beta))[d - (t+d)\beta]\alpha - 2\omega_m d\beta)^2\} \quad (9)$$

The appearance condition of magnetostatic wave instability $\beta_2\gamma<0$ is defined by its dispersion law. In limit $k_d \ll 1$, $m_z \approx M_0 - M_0|A|^2$ and $\omega_m \approx (1-|A|^2)$ we have

$$\gamma = \left.\frac{d\omega}{d|A|^2}\right|_{A=0} = -\frac{\omega_m}{4}\alpha(1-\beta) - \\ - \frac{\{\omega_m\omega_h[2+\alpha(1-\beta)] + \frac{\omega_m^2}{4}[(2+\alpha)^2 - \beta\alpha^2](1-\beta)\}}{2\{\frac{\omega_m^2}{4}[(2+\alpha)^2 - \beta\alpha^2](1-\beta) + 2\omega_m\omega_h[2+\alpha(1-\beta)]\}^{\frac{1}{2}}} \quad (10)$$

VII. CONCLUSIONS

It is established that magnetic absorption spectrum of (Ni, Zn)FeO is in frequency interval from 26 GHz to 32 GHz. The obtained theoretical calculation results of surface magnetostatic wave characteristics (SMW) in Ni-Zn ferrite-dielectric-aluminum structure confirm the experimental investigation results.

REFERENCES

[1] V.I. Zubkov, V.I. Shcheglov, "Radio Techniques I", Electronics, Vol. 52, No. 6, pp. 701-711, 2007 (in Russian).
[2] A.K. Zvezdin, A.F. Popkov, "Contribution to the Nonlinear Theory of Magnetostatlc Spin Waves", Journal of Experimental and Theoretical Physics, Vol. 57, No. 2, p. 350, 1983 (in Russian).
[3] V.I. Karpman, "Nonlinear Waves in Dispersive Media", Science Publishing House, Moscow, Russia, p. 175, 1973 (in Russian).
[4] A.D. Boardman, S.A. Nikitov, Phys. Rev. B, Vol. 38, pp. 11444-11451, 1988.
[5] A.D. Boardman, S.A. Nikitov, N.A. Waby, Phys. Rev. B, Vol. 48, p. 13602, 1993.
[6] A.D. Boardman, S.A. Nikitov, K. Xie, H.J. Mehta, Magn. and Magn. Mater., Vol. 145, p. 357, 1995.
[7] T.R. Mehdiyev, A.M. Hashimov, N.R. Babayeva, A.A. Habibzade, "Electric and Magnetic Properties of Frequency Dependent Resistor Shell", Journal of Physics, Baku, Azerbaijan, No. 3, Vol. XIV, pp. 207-217, 2008 (in Russian).
[8] E.V. Gorter, UFN, Vol. LVII, No. 2, p. 279, 1955 (in Russian).
[9] L. Neel, P. Brochet, Comptes Rendus, Vol. 230, pp. 280-282, 1950.
[10] S.V. Vonsovsky, Magnetism, Science Publishing House, Moscow, Russia, pp. 1032, 1971 (in Russian).
[11] A.B. Rinkevich, V.V. Ustinov, M.I. Samoylovich, A.F. Belyanin, S.M. Klesheva, E.A. Kuznetsov, Technologies and Constructive Electronics Apparatus, No. 4b, p. 55, 2008 (in Russian).
[12] V.P. Lukomskii, Ukrainian Physics Journal, Vol. 23, No. 1, p. 134, 1978 (in Russian).
[13] A.O. Korotkevich, S.A. Nikitov, "Cross Phase Modulation of Surface Magnetostatic Spin Waves", Journal of Experimental and Theoretical Physics, Vol. 89, No. 6, p. 205, December 1999 (in Russian).
[14] A.V. Kokin, S.A. Nikitov, "Effect of Continuous Injection on the Distribution of Envelope Solutions magnetostatic Spin Waves", FTT, Vol. 43, No. 5, pp. 851-854, 2001 (in Russian).
[15] M.A. Malugina, U.P. Sharaevskii, Izv. Vuzov, Applied Nonlinear Dynamics, Vol. 8, No. 3, pp. 59-69, 2000 (in Russian).
[16] G.M. Dudko, M.A. Malugina, U.P. Sharaevskii, Izv. Vuzov, Applied Nonlinear Dynamics, Vol. 8, No. 6, 2003 (in Russian).
[17] A.D. Bordman, K. Xie, Phys. Rev. Lett., Vol. 75, No. 25, p. 4591, 1995.
[18] R. Marcelli, S.A. Nikitov, Europhys. Lett., Vol. 54, No. 1, pp. 91-97, 2001.
[19] A.S. Kindyak, Pisma and Journal of Experimental and Theoretical Physics, Vol. 25, No. 4, pp. 48-54, 1999 (in Russian).
[20] A.S. Kindyak, JTF, Vol. 69, No. 6, p. 119, 1999 (in Russian).
[21] B.A. Knyazev, A.V. Kuzmin, "Surface Electromagnetic Waves: Basic Properties, Building, Transportation", IYAF Im. G.I. Budkera SO RAN, Novosibirsk, p. 26, 2003 (in Russian).

BIOGRAPHIES

Shahla N. Aliyeva was born in Baku, Azerbaijan in May 1985. She works in Institute of Physics, Azerbaijan National Academy of Sciences, Baku, Azerbaijan from 2009. Currently, she is a Ph.D. student and works at Laboratory of Molecular Spectroscopy of the same institute. She has three scientific publications.

S.I. Aliyeva was born in Baku, Azerbaijan on January 21, 1971. She works in Institute of Physics, Azerbaijan National Academy of Sciences, Baku, Azerbaijan from 1994. Currently, she is a Scientific Investigator at Department of Modern Information System of the same institute. She has three scientific publications.

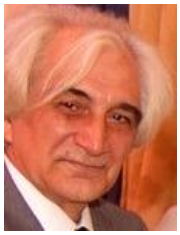

Talat R. Mehdiyev was born in Baku, Azerbaijan on June 4, 1944. He works in Institute of Physics, Azerbaijan National Academy of Sciences, Baku, Azerbaijan from 1964. He is a Professor of Physics from 1992 and Head of Department of at the same institute from 1975 and also editor of Azerbaijan Scientific Journal of Physics from 1994.